# Improved Moments Estimation for VHF Active Phased Array Radar Using Fuzzy Logic Method

S. ALLABAKASH

*Department of Physics, Sri Venkateswara University, Tirupati, India*

P. YASODHA

*National Atmospheric Research Laboratory, Department of Space, Government of India, Gadanki, India*

L. BIANCO

*Cooperative Institute for Research in Environmental Sciences, University of Colorado Boulder, and NOAA/Earth System Research Laboratory/Physical Sciences Division, Boulder, Colorado*

S. VENKATRAMANA REDDY

*Department of Physics, Sri Venkateswara University, Tirupati, India*

P. SRINIVASULU

*National Atmospheric Research Laboratory, Department of Space, Government of India, Gadanki, India*

(Manuscript received 17 March 2014, in final form 22 October 2014)

ABSTRACT

Various nonatmospheric signals contaminate radar wind profiler data, introducing bias into the moments and wind velocity estimation. This study applies a fuzzy logic–based method to Doppler velocity spectra to identify and eliminate the clutter echoes. This method uses mathematical analyses and a fuzzy inference system applied to each Doppler velocity spectrum to separate the atmospheric signals from the clutter. After eliminating the clutter, an adaptive algorithm is used to estimate mean Doppler velocities accurately. This combination of techniques is applied to the spectral data obtained by the newly developed 53-MHz active phased array radar located at the National Atmospheric Research Laboratory (NARL), Gadanki, India (13.5°N, 79°E). Winds derived using the conventional method and the method developed for this study are compared with those obtained by collocated GPS radiosonde. The comparison shows that the present method derives the winds more accurately compared to the conventional method.

## 1. Introduction

Radar wind profilers (RWPs) are powerful remote sensing instruments for measuring atmospheric wind velocities and turbulence (Gage and Balsley 1978; Balsley and Gage 1982). Profiler data are used in weather forecasting, climate modeling, natural hazards identification (forecasting), nowcasting, air traffic control (Merritt 1995), etc. Therefore, maintaining high data quality is very important. RWPs employ a Doppler beam swinging (DBS) technique, in which the narrow radar beam is switched sequentially in a fixed routine between three and five noncoplanar directions (one vertical zenith, and two or four off vertical in orthogonal directions). RWPs radiate an electromagnetic signal and receive the backscattered echo from the refractive index irregularities present in the atmosphere and advected by the wind. Thus, the received backscattered signal will have a shift in the frequency. Backscatter from the clear-air turbulence is a weak scattering mechanism. Thus, the received atmospheric signal is very weak. Further, the received signal is often contaminated by the ground clutter generated from stationary nonatmospheric

*Corresponding author address:* S. Venkatramana Reddy, Department of Physics, Sri Venkateswara University, Tirupati 517 502, Andhra Pradesh, India.
E-mail: drsvreddy123@gmail.com

DOI: 10.1175/JTECH-D-14-00075.1

targets and intermittent clutter generated by the moving nonatmospheric targets (birds, airplanes, etc.). The shift of the Doppler frequency in the atmospheric echoes is used to estimate the wind velocity. Hence, the data must be processed with care to estimate the mean Doppler shift; if they are contaminated by clutter signal, which is generally stronger than the atmospheric signal, then the velocity estimates can be wrong.

Conventional signal processing techniques for the wind profilers are given by Barth et al. (1994), Strauch et al. (1984), Riddle and Angevine (1992), Passarelli et al. (1981), Wilczak et al. (1995), and Carter et al. 1995. For VHF radars, conventional DC[1] removal techniques from power spectrum data involve three-point or five-point DC removal (Barth et al. 1994), where the DC component of the data is replaced with the averaged value of the data corresponding to one (three-point DC removal) or two (five-point DC removal) adjacent points on either side. This technique is not suitable for removing clutter, which extends for several Doppler bins around DC. A linear interpolation is used in such cases where a few data points on either side of DC are replaced with interpolated data values. However, this technique is not effective in situations where the Doppler frequency of the atmospheric signal is close to zero and overridden by the clutter. In such cases, eliminating the clutter using interpolation will eliminate the desired atmospheric signal as well, thus causing a serious problem in mean Doppler velocity estimation. Further, this process will not eliminate intermittent clutter. Even wavelet-transform-based processing techniques (Jordan et al. 1997; Lehmann and Teschke 2001; Lehtinen and Jordan 2006) mitigate the clutter contamination only to some extent. Lehtinen and Jordan (2006) used wavelet filtering with a multiple-peak picking algorithm [Swiss Federal Institute of Technology (ETH) MPP method] and Anandan et al. (2005) used an adaptive moments estimation method for calculating moments, which improves the accuracy.

In recent years, a new approach was developed based on fuzzy logic (FL) to identify and remove the contamination from wind profiler range–Doppler spectral data, and this was proven to be an effective technique to remove clutter. We have used a FL-based technique to eliminate the undesired signal from the data collected by a VHF active phased array radar wind profiler, located at NARL. The FL method presented by Cornman et al. (1998), Morse et al. (2002), and Bianco and Wilczak (2002) is adjusted and tuned according to the characteristics of the signal and site location. Further, an adaptive moments estimation (Anandan et al. 2005) method is implemented for the identification of the peak and the estimation of the moments on the cleaned spectra. In section 2 we present the FL method and approach utilized in this study, while the results obtained by the conventional method compared with the results obtained by the one developed here are presented in section 3. Conclusions are presented in the last section.

TABLE 1. Important specifications of the system.

| Parameter | Value |
|---|---|
| Frequency | 53 MHz |
| Technique | Doppler Beam Swinging |
| Number of beams | 5 (east, west, zenith, north, south) |
| Peak power | 133 kW at 10% duty ratio |
| Antenna | 133 elevation array (50 m) |
| Bandwidth | 3.4 MHz |
| Pulse width | 1–64 $\mu$s |
| Max range coverage | 10–12 km |
| Range resolution | 150 m |
| Time resolution | 3 min (for one set of five beam directions) |

## 2. Dataset and analysis

Data collected by the VHF active phased array radar during 2013 are used in this study. This radar operates at 53 MHz and has a 133-element antenna array arranged in seven groups, with each group comprising 19 elements. Each antenna element is excited with a 1-kW transmit–receive module, and the peak power of the radar is 133 kW at a maximum duty ratio of 10%. This radar is used for probing the atmosphere up to about 10–12 km. For more details about the system, readers can refer to Srinivasulu et al. (2013). Important specifications of the radar are given in Table 1.

Figure 1a schematically shows a representation of the conventional signal processing steps involved in wind velocity estimation. First, coherent integration (Barth et al. 1994; Carter et al. 1995) is performed on the complex received signal (inphase: I signal, quadrature phase: Q signal) to improve the signal-to-noise ratio and reduce the data volume. Then the signal is transformed into the frequency domain using complex Fourier transform. To reduce spectral leakage and picket fence effects, windowing (generally Hamming or Hanning) is applied. The power spectrum is computed and three- or five-point DC removal or linear interpolation is implemented. Several successive spectra are incoherently averaged to improve the detectability. The mean noise

[1] DC refers to the zero frequency on the Doppler frequency axis. Because the clutter signal, which contaminates the radar backscatter, is due to stationary targets, it appears at zero frequency on the Doppler axis.

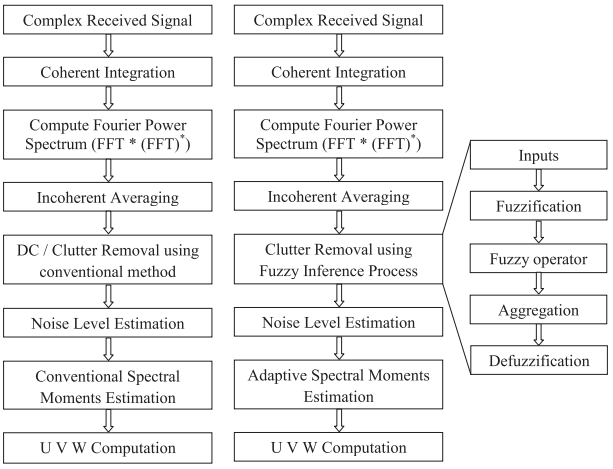


FIG. 1. (a) Classical signal processing steps for wind velocity measurement. (b) Signal processing steps for wind velocity measurement using the FL method. (c) Fuzzy logic inference process flow.

level is computed using the Hildebrand and Sekhon method (Hildebrand and Sekhon 1974) and subtracted from the Doppler spectrum before moments (Woodman 1985) and wind velocities (Sato 1989) are calculated. As the DC removal or interpolation does not remove the contamination in the atmospheric data due to clutter, the estimated winds may be in error when using the conventional signal processing.

The schematic representation of the FL approach of analyzing data (Klir and Yuan 1997; Zadeh 1965) is shown in Fig. 1b. The main difference between the conventional signal processing approach and the FL signal processing approach is in the removal of clutter/DC. In the FL approach, after incoherent averaging, the range–Doppler spectra are subjected to a fuzzy inference process to remove the clutter contamination. Fuzzy inference is the process of formulating the mapping from a given input to an output using FL. Figure 1c schematically illustrates the steps involved in the fuzzy inference process. This process consist of 1) *fuzzification* of the input variables, 2) application of the fuzzy operator (*AND* or *OR*), 3) aggregation of the consequents across the rules, and 4) *defuzzification*. The fuzzification step takes the normalized parameters as inputs and converts them through membership functions. The outputs of the fuzzification step are values always in the interval between 0 and 1. The fuzzy operator step takes two or more membership values (fuzzified inputs) and generates the single truth value depending on the operators. Generally AND (minimum or product) or OR (maximum or sum) are used as fuzzy operators. The aggregation method takes all the truth membership values produced by fuzzy operators as inputs. Three methods—1) *max* (maximum), 2) *probor* (probabilistic OR), and 3) *sum* (simply the sum of each rule's output value)—are used in the aggregation process to generate a resultant membership value. This output membership value of the aggregation process acts as the input for the defuzzification. In the defuzzification process, different methods like centroid, bisector, middle of maximum, largest value of maximum, and smallest of maximum are used. For details on these methods, readers can refer to the MATLAB fuzzy logic toolbox (Mathworks 2013) or Sivanandam et al. (2007). Among these methods, the centroid method is widely used. In this paper we use the centroid defuzzification method, which picks up the center of the area under the curve.

The fuzzy logic attributes are estimated across the Doppler velocity spectrum before estimating the

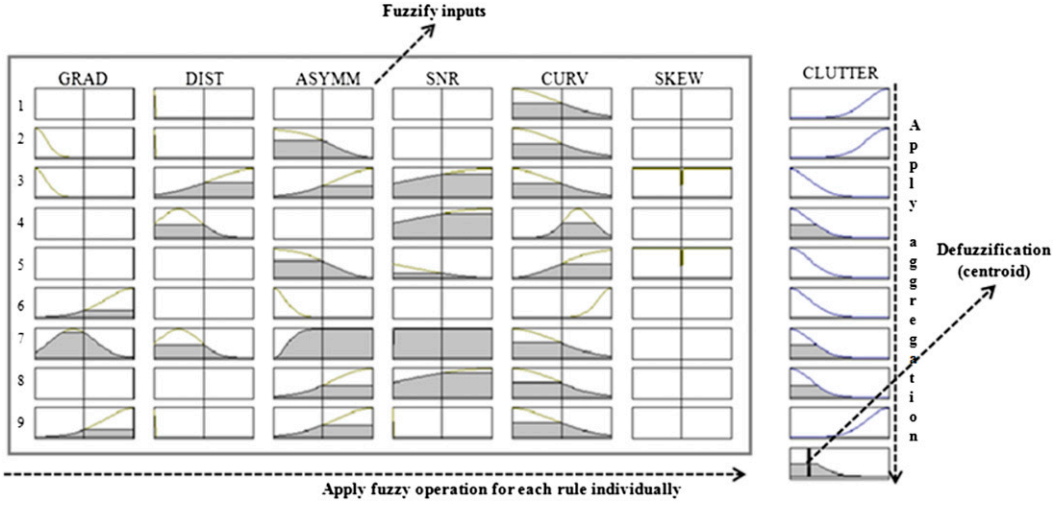


FIG. 2. Fuzzy inference process for clutter.

spectral moments. The mathematical parameters of the data, such as power spectral density (PSD), signal-to-noise ratio (SNR), asymmetry, curvature, skewness, and gradient, are computed as given by Cornman et al. (1998), Bianco and Wilczak (2002), and Morse et al. (2002) after the incoherent averaging. These parameters are used to differentiate the atmospheric signal from the clutter. We have used the MATLAB fuzzy logic toolbox R2013b (Mathworks 2013) for developing the tool aimed at the identification of clutter and atmospheric signal. The fuzzy inference process for clutter recognition is represented in Fig. 2. Using the fuzzification process, membership functions are calculated for these normalized mathematical parameters. Backscattered signal characteristics are different for various atmospheric conditions, topography, and radar parameters (Morse et al. 2002). Thus, the membership functions and rules as tuned (modified) for identifying atmospheric signal and clutter signal are not the same for all the radar sites. Therefore, the membership function values and rules, as tuned (modified) for the NARL location and radar signal characteristics, are given as tables A1 through A13 in the appendix. The tuning process is carried out according to Cornman et al. (1998), Bianco and Wilczak (2002), and Morse et al. (2002), where suitable membership functions and their mathematical parameters that recognize the features of the atmospheric backscattered signal are identified. For the study presented here, the membership functions found suitable for the identification of clutter (clutt) and atmospheric signal (atm) are Gaussian shaped, Π shaped and trapezoidal shaped. To identify the mathematical parameter values for these functions, trial and error basis experimentation were carried out on large set of data and suitable values were found empirically.

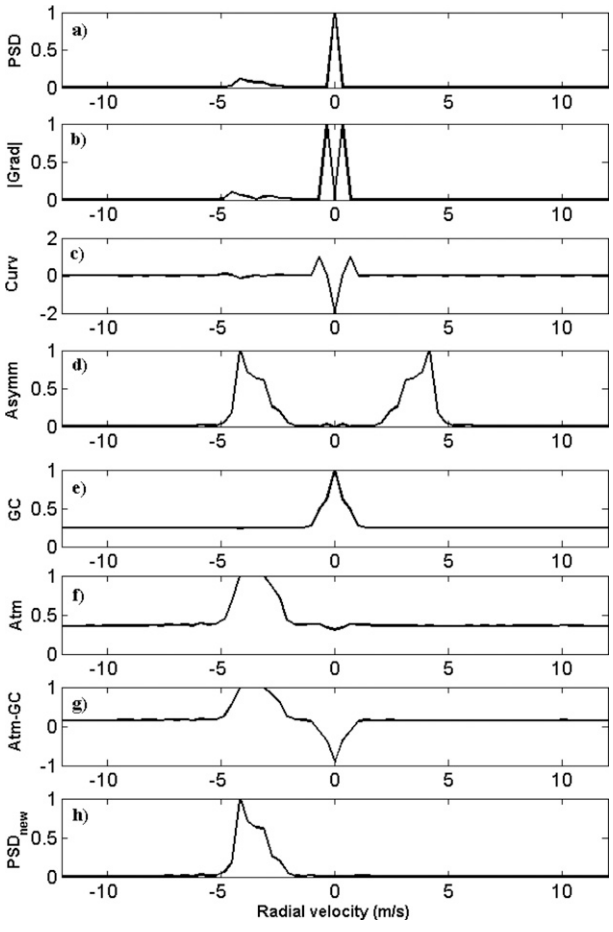


FIG. 3. Normalized mathematical parameters: (a) original power spectrum, (b) gradient, (c) curvature, (d) asymmetry, (e) clutter score, (f) atmospheric score, (g) total score (clutter score is subtracted from atmospheric score), and (h) processed power spectrum.

Once the clutter is removed from the Doppler spectra, the data are subjected to the moments estimation algorithm, where signal power, mean Doppler shift, and spectral width are estimated. The conventional method to estimate the mean Doppler shift selects the dominant peak in the Doppler power spectrum as the atmospheric signal. This method fails particularly in the upper heights, where the noise is comparably stronger than the atmospheric signal and also at heights where multiple peaks are present. In such cases, the conventional method picks the wrong signal as the atmospheric one. To circumvent this possibility, an adaptive algorithm (Anandan et al. 2005) is used instead, which selects the desired atmospheric signal peak using some predefined criteria for parameters such as the Doppler window, the wind shear threshold, and the signal-to-noise ratio based on spatial and temporal continuity. As a result, the adaptive method can pick the desired atmospheric signal in all such cases (noisy regions and presence of multiple peaks) where the conventional moments estimation algorithm fails.

In the adaptive method algorithm, a Doppler window is fixed, typically with a width equal to 20% of the entire Doppler axis width. As a first step, the mean Doppler frequency of the atmospheric signal peak, after removal of the clutter, is identified for the first range gate. For the second range gate, the search to locate the signal peak is carried out within the fixed Doppler window centered on the mean Doppler frequency of the first range gate, whose SNR is above 7 dB (and below max SNR). For the third range gate, the Doppler window is centered on the mean Doppler frequency of the signal identified for the second range gate, and so on. This process is repeated until the last range gate, having provided a predefined Doppler window for the identification of the signal. More details on this algorithm are given in Anandan et al. (2005).

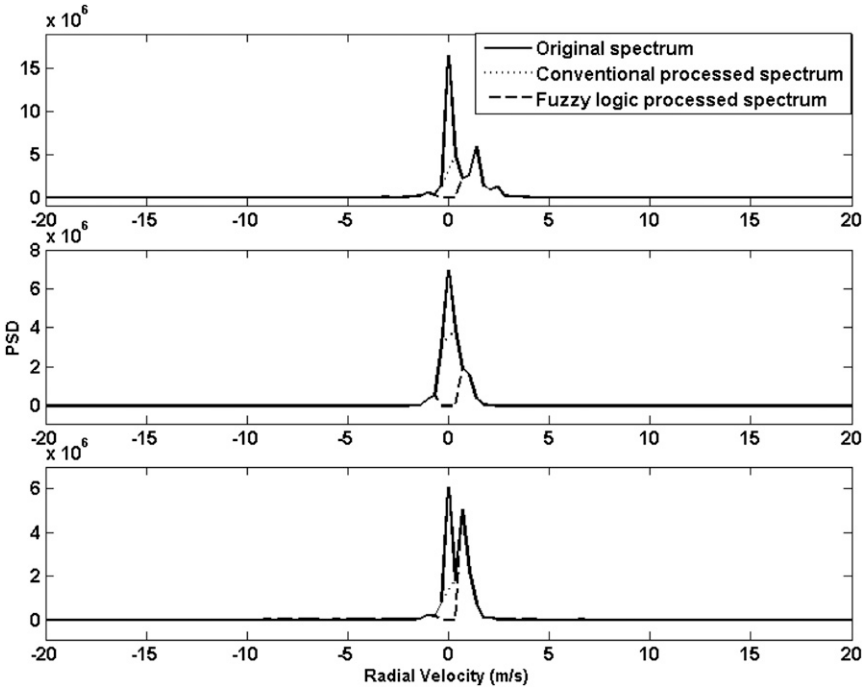


FIG. 4. Example spectra where atmospheric signal and clutter overlap.

## 3. Results and discussion

The power spectrum of a single range gate, where the clutter is dominating over the atmospheric signal, is chosen for explaining the FL processing technique. Figure 3 shows the normalized parameters. The original power spectrum, where strong ground clutter (GC) is present at the zero frequency and the desired weak atmospheric (atm) signal is located to its left, is shown in Fig. 3a. The absolute gradient calculated for this spectrum is shown in Fig. 3b. The value of the gradient is small at the peak portion of the clutter and atmospheric signal and large at their edges. The curvature calculated for all the spectral points is shown in Fig. 3c. The value of the curvature at the peak of the clutter is smaller (a more negative value) compared to the value at the peak of the atmospheric signal. Further, it is larger (positive value) at the edges of the clutter compared to the value at the edges of the atmospheric signal. The asymmetry computed for all the points in the spectrum is shown in Fig. 3d. This is the absolute value of the difference between the positive ($+f$) and negative ($-f$) Doppler frequency points, located on either side of the zero frequency point. Figures 3e and 3f show the clutter score and the atmospheric signal score obtained by the FL processing technique. The clutter score is large where the clutter is actually present and the atmospheric score is large where the atmospheric signal is actually present. Finally, we subtract the clutter score from the atmospheric score and the resultant atm–GCs shown in Fig. 3g. From this figure we can observe that the clutter-dominated portion of the spectra becomes negative and the atmospheric signal-dominated part is positive. The area where these values are negative is replaced with random noise values in the original spectrum (Bianco and Wilczak 2002). Finally, the processed-cleaned spectrum is shown in Fig. 3h.

Figure 4 shows power spectra for three different range gates presenting different types of clutter contamination of the backscattered signal. The original power spectrum, the processed spectrum using the conventional method, and the processed spectrum using the FL algorithm are represented by solid, dotted, and dashed lines, respectively, in all three panels of the figure. In the top panel the clutter and atmospheric signals are close to each other and the clutter signal is stronger compared to the atmospheric signal. In the middle panel, the clutter signal is overriding the atmospheric signal. In the bottom panel, the clutter and atmospheric signals are close to each other and their powers are almost equal. In all three cases, the conventional method with five-point DC removal does not completely eliminate the clutter, as can be seen in the figure. However, it can be seen that the FL algorithm has eliminated the clutter completely, leaving only the atmospheric signal.

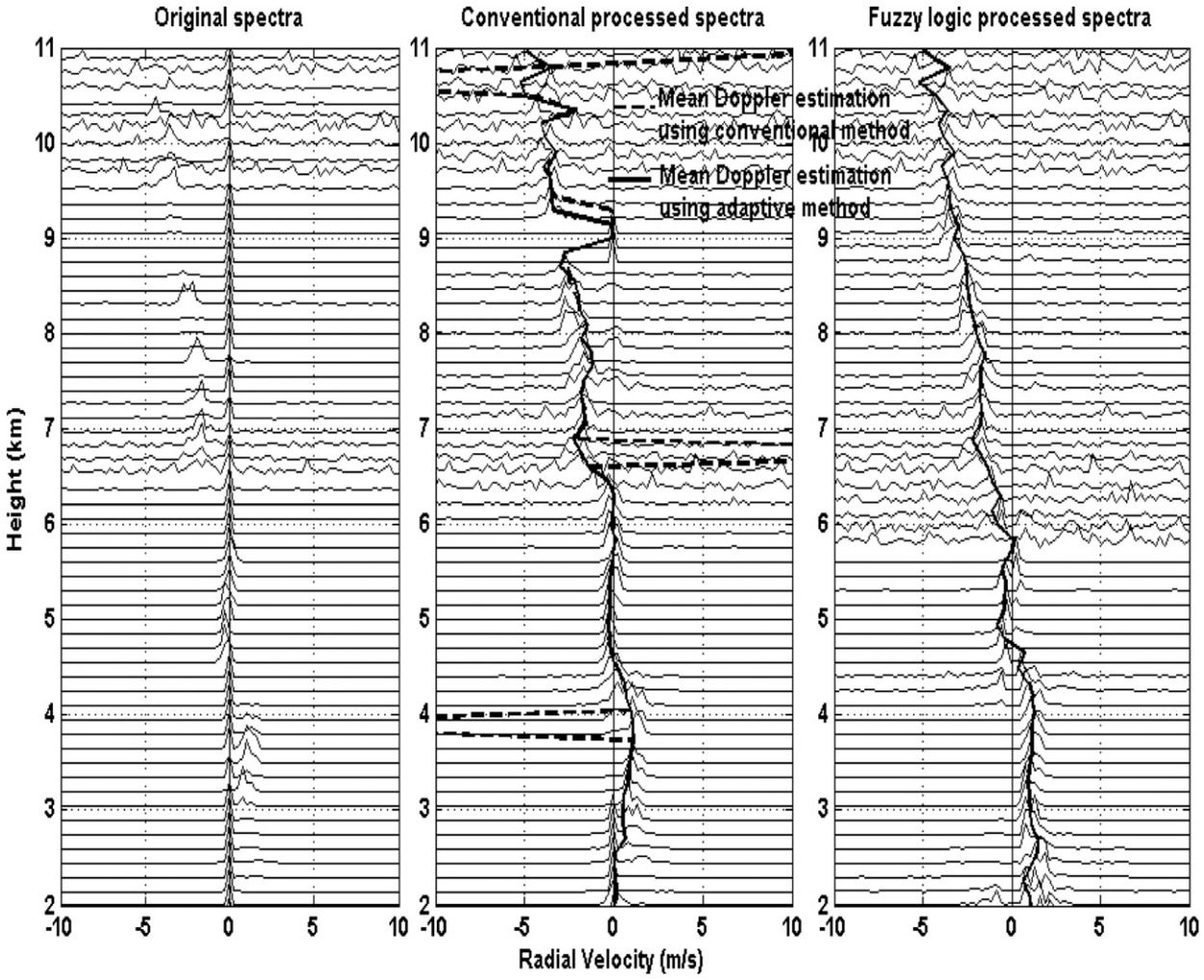


FIG. 5. West beam: (left) the original spectra for all range gates, (middle) processed spectra using the conventional five-point DC removal method, and (right) processed spectra using the FL technique. The mean Doppler shift estimated using the conventional moments estimation method and the adaptive moments estimation method are shown as dashed and solid lines, respectively, on the processed data in the middle panel.

Figure 5 shows the range–Doppler spectra for the west beam, observed by the radar at 1700 local time (LT) 7 August 2013. The left panel shows the original spectra, the middle panel shows the processed spectra using the conventional five-point DC removal method, and the right panel shows the processed spectra using the FL technique. The mean Doppler shift estimated using the conventional moments estimation method and the adaptive moments estimation method are shown as dashed and solid lines, respectively, on the conventionally processed data. In the right panel, the solid line indicates the mean Doppler shift estimated using the adaptive moments estimation method. From the figure, it is evident that the conventional method with five-point DC removal still leaves a portion of the clutter signal that is closer to the atmospheric signal in some range gates. Further, it can also be seen that even if we apply the adaptive moments estimation algorithm to the conventionally processed data, it is difficult to pick the atmospheric peak due to the following reasons: (i) the clutter signal amplitude is still stronger compared to the atmospheric signal and (ii) both are very close to each other. However, in the FL-processed spectrum (right panel), the clutter is completely eliminated and thus the adaptive moments estimation algorithm can pick the atmospheric signal peak, based on the knowledge obtained from the data in the previous range gate. As a result, the mean Doppler velocity can be estimated more accurately.

A comparison plot between the wind profiles derived by the radar (processed by the FL method as well as conventional method) for the same data that are used in

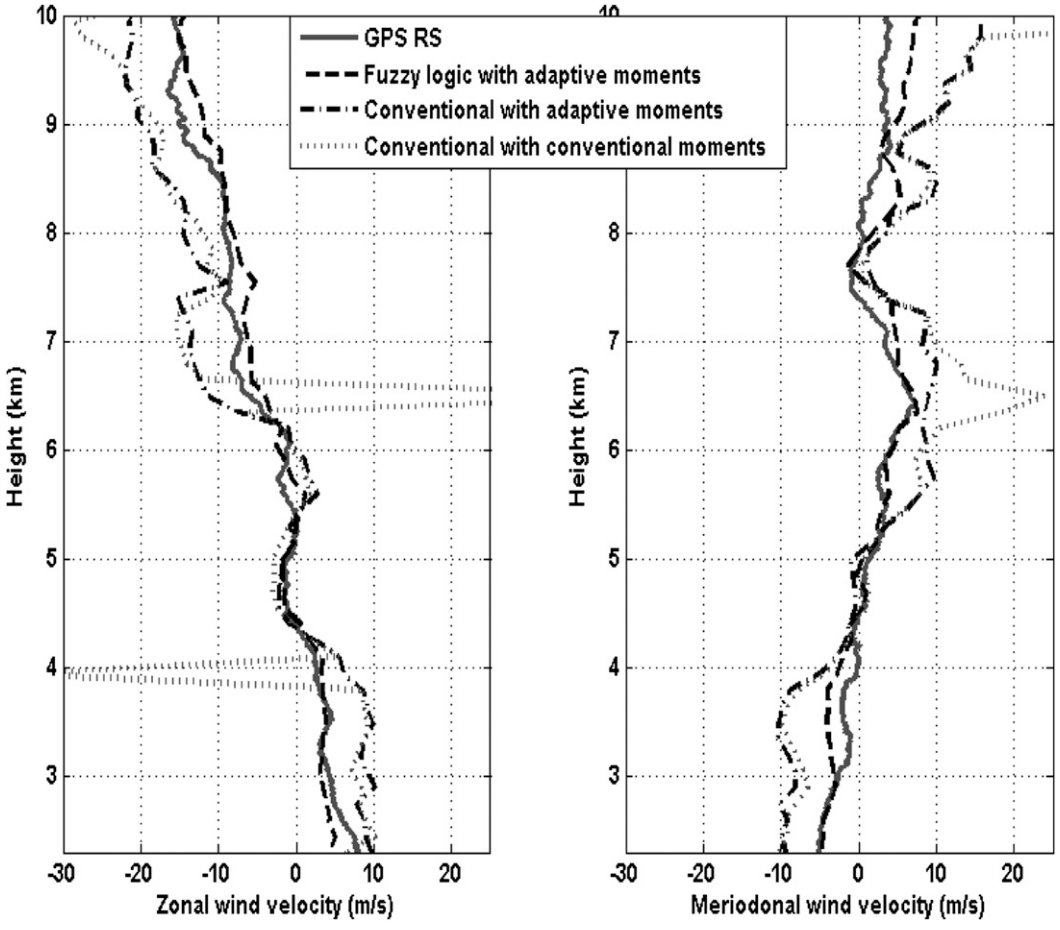


FIG. 6. Wind velocity components $U$ and $V$ derived using GPS RS (solid lines) and radar observations. Radar winds are processed using the conventional method with conventional moments estimation (dashed lines), conventional method with adaptive moments estimation (dashed–dotted lines), and FL method with adaptive moments estimation (dotted lines).

Fig. 5 and the collocated GPS radiosonde (GPS RS) is shown in Fig. 6, where we note that the fuzzy-derived winds are in good agreement with GPS RS–derived wind velocities. The left and right panels illustrate the zonal and meridional wind velocities, respectively. To verify the validity of this method, we tested the FL tool on the radar data over a large number of observations available over a time period of 10 months. For this extended dataset, scatterplots of the zonal ($U$) and meridional ($V$) wind components were constructed, showing the comparison between winds derived from the GPS RS and those from RWP using 1) the conventional processing method with five-point DC removal and conventional moments estimation, 2) the conventional processing method with adaptive moments estimation, and 3) the FL processing method with adaptive moments estimation (Figs. 7–9, respectively, where solid lines in all plots are the best-fit linear interpolation of the data). It may be noted that the correlation coefficients for the zonal- and meridional-derived winds are 0.72 and 0.68, respectively, in the first case (Fig. 7); 0.83 and 0.78, respectively, in the second case (Fig. 8); and 0.95 and 0.90, respectively, in the third case (Fig. 9). From this comparison it is evident that the FL method combined with the adaptive moments estimation algorithm is efficient at identifying the real atmospheric signal and deriving spectral moments.

## 4. Conclusions

We tested a tuned fuzzy logic method to remove contaminated signal from the data collected by VHF active phased array radar during 2013. Results from this study demonstrate that this method is successful at removing the clutter signal in the received signal. The combination of FL and adaptive moments estimation methods reduces clutter contamination and effectively identifies the desired signal. We verified that the

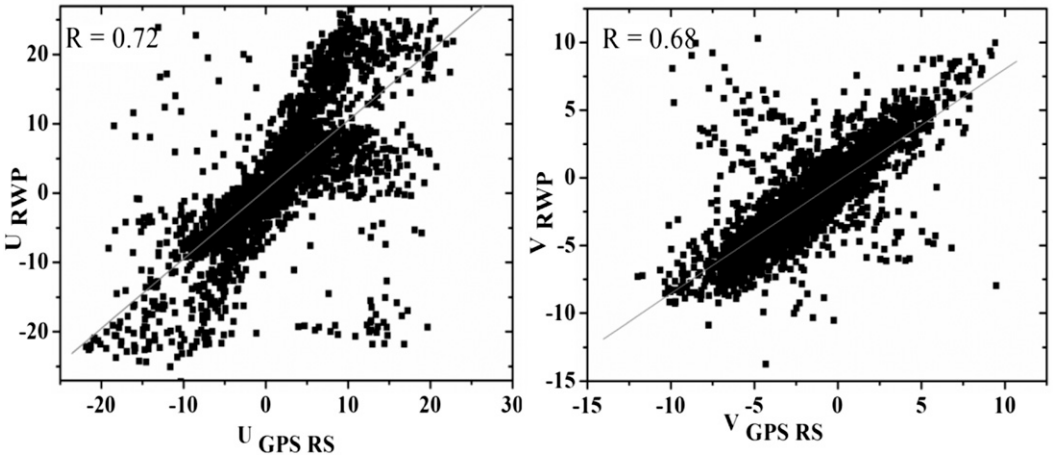


FIG. 7. Scatterplot of the *U* and *V* wind components showing the correlation between winds derived from GPS RS and those derived from radar. Radar winds were processed using the conventional method with conventional moments estimation.

proposed method is able to effectively separate the atmospheric signal, even when clutter and atmospheric signals are overlapping each other, resulting in more accurate estimations of wind speeds compared to the conventional processing method. We tested this method on a 10-month-long dataset and the results are found to be satisfactory. The wind velocities derived using this method are compared with the collocated GPS radiosonde, yielding very good correlation and suggesting that the method presented in this study is effective.

*Acknowledgments.* The authors thank James M. Wilczak, of the NOAA/Earth System Research Laboratory/Physical Sciences Division, Boulder, Colorado, for his valuable suggestions and advice. We also thank three anonymous reviewers and the editor for their insightful comments that improved the manuscript.

## APPENDIX

### Fuzzy Logic Membership Functions and Rules

Three distinct membership function types are used: Gaussian, Π shaped, and trapezoidal, defined as follows:

Gaussian membership function:

$$f(\mathbf{x};\sigma,c) = \exp\left[\frac{-(\mathbf{x}-c)^2}{2\sigma^2}\right].$$

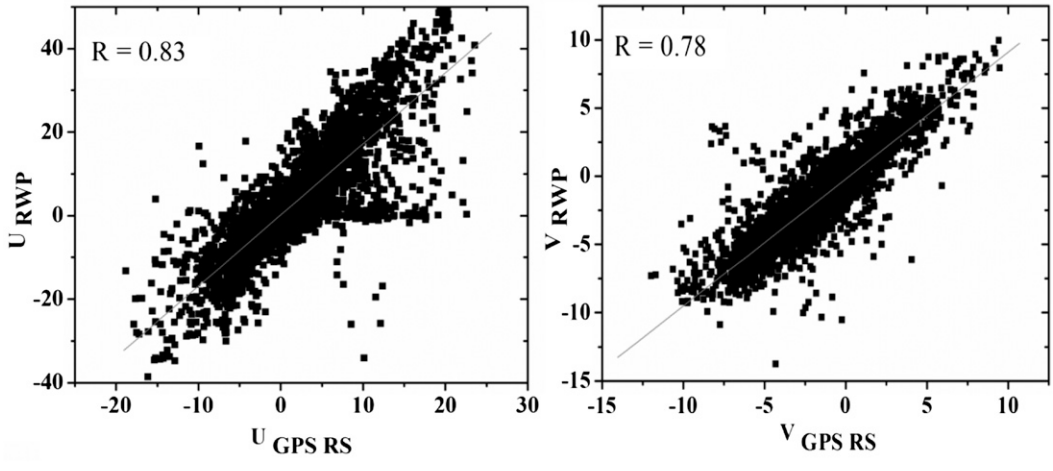


FIG. 8. Scatterplot of the *U* and *V* wind components showing the correlation between winds derived from GPS RS and those derived from radar. Radar winds were processed using the conventional method with adaptive moments estimation.

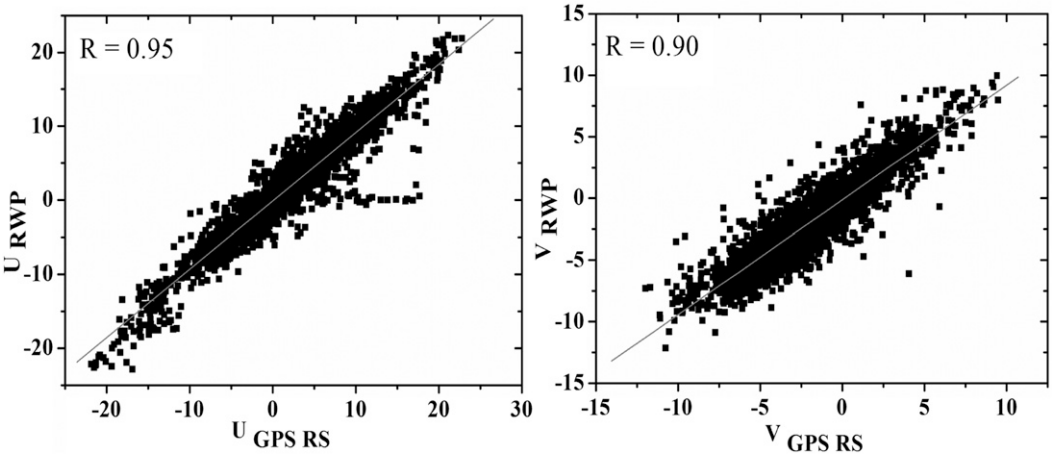


FIG. 9. Scatterplot of the $U$ and $V$ wind components showing the correlation between winds derived from GPS RS and those derived from radar. Radar winds were processed using the FL method with adaptive moments estimation.

Π shaped:

This is a spline-based curve, so named because of its Π shape. The membership function is evaluated at the points determined by the vector **x**:

$$f(\mathbf{x};a,b,c,d)=\begin{cases}0, & \mathbf{x}\le a\\ 2\left(\dfrac{\mathbf{x}-a}{b-\mathrm{a}}\right)^2, & \mathrm{a}\le\mathbf{x}\le\dfrac{\mathrm{a}+\mathrm{b}}{2}\\ 1\text{-}2\left(\dfrac{\mathbf{x}-\mathrm{b}}{\mathrm{b}-\mathrm{a}}\right)^2, & \dfrac{\mathrm{a}+\mathrm{b}}{2}\le\mathbf{x}\le\mathrm{b}\\ 1, & \mathrm{b}\le\mathbf{x}\le\mathrm{c}\\ 1\text{-}2\left(\dfrac{\mathbf{x}-\mathrm{c}}{\mathrm{d}-\mathrm{c}}\right)^2, & \mathrm{c}\le\mathbf{x}\le\dfrac{\mathrm{c}+\mathrm{d}}{2}\\ 2\left(\dfrac{\mathbf{x}-\mathrm{d}}{\mathrm{d}-\mathrm{c}}\right)^2, & \dfrac{\mathrm{c}+\mathrm{d}}{2}\le\mathbf{x}\le\mathrm{d}\\ 0, & \mathbf{x}\ge\mathrm{d}\end{cases}.$$

Trapezoidal:

$$\mathrm{f}(\mathbf{x};\mathrm{a},\mathrm{b},\mathrm{c},\mathrm{d})=\max\left[\min\left(\frac{\mathbf{x}-\mathrm{a}}{\mathrm{b}-\mathrm{a}},1,\frac{\mathrm{d}-\mathbf{x}}{\mathrm{d}-\mathrm{c}}\right),0\right].$$

These membership functions are shown in Tables A1 through A7.

More membership functions and parameters are given in Tables A8 through A13.

*a. Clutter recognition algorithm*

For all the mathematical parameters (gradient, distance, asymmetry, SNR, curvature, skewness) and clutter output, Gaussian membership functions are computed and the shape depends on parameters $c$ and $\sigma$, which represent the center and width of the curve, respectively. Parameter values ($c$ and $\sigma$) and rules depend on signal characteristics and site location.

CLUTTER RULES

1) If the distance from zero radial velocity is small and curvature is negative, then clutter is large.
2) If the gradient is small and distance from zero radial velocity is small and asymmetry is not large and curvature is negative, then clutter is large.
3) If the gradient is small and distance from zero radial velocity is large and asymmetry is large and SNR is large and curvature is negative and skewness is not zero, then clutter is small.
4) If the distance from zero radial velocity middle and SNR is large and curvature is zero, then clutter is small.

TABLE A1. Gradient membership functions and parameters used for the clutter recognition.

| Membership function | Function | Parameter | Parameter |
|---|---|---|---|
| Small | Gaussian | $\sigma = 110$ | $c = 13.26$ |
| Middle | Gaussian | $\sigma = 210$ | $c = 392$ |
| Large | Gaussian | $\sigma = 300$ | $c = 1002$ |

TABLE A2. Distance membership functions and parameters used for the clutter recognition.

| Membership function | Function | Parameter | Parameter |
|---|---|---|---|
| Small | Gaussian | $\sigma = 7.5$ | $c = 2.5$ |
| Middle | Gaussian | $\sigma = 199$ | $c = 247$ |
| Large | Gaussian | $\sigma = 437.5$ | $c = 1000$ |

TABLE A3. Asymmetry membership functions and parameters used for the clutter recognition.

| Membership function | Function | Parameter | Parameter |
|---|---|---|---|
| Small | Gaussian | $\sigma = 130$ | $c = 0$ |
| Middle | Gaussian | $\sigma = 170$ | $c = 349$ |
| Large | Gaussian | $\sigma = 380$ | $c = 1000$ |

TABLE A4. SNR membership functions and parameters used for the clutter recognition.

| Membership function | Function | Parameter | Parameter |
|---|---|---|---|
| Small | Gaussian | $\sigma = 4.717$ | $c = 1.09 \times 10^{-13}$ |
| Large | Gaussian | $\sigma = 834.6$ | $c = 989.9$ |

5) If the asymmetry is not large and SNR is not large and curvature is not negative and skewness is not zero, then clutter is small.
6) If the gradient is large and asymmetry is small and curvature is positive, then clutter is small.
7) If the gradient is middle and distance from zero radial velocity is middle and asymmetry is not small and SNR is not small and curvature is negative, then clutter is small.
8) If the asymmetry is large and SNR is large and curvature is negative, then clutter is small.
9) If the gradient is large and distance is small and asymmetry is large and SNR is small and curvature is negative, then clutter is large.

### *b. Wind (atmospheric signal) recognition algorithm*

In the wind recognition algorithm, the gradient, SNR, asymmetry, distance, and wind output are computed using Gaussian membership functions. For computing the curvature, (negative and positive) the Π-shaped (the parameters *a* and *d* locate the left and right, respectively, base points or "feet" of the curve; the parameters *b* and *c* set the left and right, respectively, top point or "shoulders" of the curve) and trapezoidal-shaped (the parameters *a* and d locate the feet of the trapezoid and the parameters *b* and *c* locate the shoulders) membership functions are used.

TABLE A5. Curvature membership functions and parameters used for the clutter recognition.

| Membership function | Function | Parameter | Parameter |
|---|---|---|---|
| Negative | Gaussian | $\sigma = 840$ | $c = -1000$ |
| Zero | Gaussian | $\sigma = 288$ | $c = 334$ |
| Positive | Gaussian | $\sigma = 274$ | $c = 994$ |

TABLE A6. Skewness membership functions and parameters used for the clutter recognition.

| Membership function | Function | Parameter | Parameter |
|---|---|---|---|
| Zero | Gaussian | $\sigma = 10$ | $c = 0$ |

TABLE A7. Clutter output membership functions and parameters used for the clutter recognition.

| Membership function | Function | Parameter | Parameter |
|---|---|---|---|
| Small | Gaussian | $\sigma = 212.3$ | $c = 0$ |
| Middle | Gaussian | $\sigma = 212$ | $c = 503$ |
| Large | Gaussian | $\sigma = 212$ | $c = 997$ |

TABLE A8. Gradient membership functions and parameters used for the wind recognition.

| Membership function | Function | Parameter | Parameter |
|---|---|---|---|
| Small | Gaussian | $\sigma = 300.2$ | $c = 0$ |
| Middle | Gaussian | $\sigma = 412.2$ | $c = 600$ |
| Large | Gaussian | $\sigma = 712.2$ | $c = 1000$ |

WIND (ATMOSPHERIC SIGNAL) RULES

1) If the gradient is small and curvature is negative and asymmetry is large and distance is large, then wind is large.
2) If the gradient is middle and SNR is small and curvature is positive and asymmetry is small and distance is large, then wind is middle.
3) If the gradient is small and SNR is large and curvature is negative and asymmetry is small, then wind is small.
4) If the asymmetry is small and distance is small, then wind is small.
5) If the gradient is middle and distance is small, then wind is small.
6) If the gradient is small and SNR is small and distance is small, then wind is small.
7) If the curvature is not negative and gradient is not small and asymmetry is small, then wind is small.

TABLE A9. SNR membership functions and parameters used for the wind recognition.

| Membership function | Function | Parameter | Parameter |
|---|---|---|---|
| Small | Gaussian | $\sigma = 9.43$ | $c = 1.1 \times 10^{-13}$ |
| Large | Gaussian | $\sigma = 800$ | $c = 10\,000$ |

TABLE A10. Curvature membership functions and parameters used for the wind recognition.

| Membership function | Function | *a* | *b* | *c* | *d* |
|---|---|---|---|---|---|
| Negative | Π shaped | −765 | −190 | −185 | 5.3 |
| Positive | Trapezoidal shaped | −0.051 | 339 | 1030 | 2400 |

TABLE A11. Asymmetry membership functions and parameters used for the wind recognition.

| Membership function | Function | Parameter | Parameter |
|---|---|---|---|
| Small | Gaussian | $\sigma = 80$ | $c = 0$ |
| Middle | Gaussian | $\sigma = 320$ | $c = 630$ |
| Large | Gaussian | $\sigma = 770$ | $c = 1000$ |

TABLE A12. Distance membership functions and parameters used for the wind recognition

| Membership function | Function | Parameter | Parameter |
|---|---|---|---|
| Small | Gaussian | $\sigma = 10$ | $c = 0$ |
| Large | Gaussian | $\sigma = 838$ | $c = 1000$ |

TABLE A13. Wind output membership functions and parameters used for the wind recognition

| Membership function | Function | Parameter | Parameter |
|---|---|---|---|
| Small | Gaussian | $\sigma = 212.3$ | $c = 0$ |
| Middle | Gaussian | $\sigma = 212$ | $c = 470$ |
| Large | Gaussian | $\sigma = 212$ | $c = 497$ |

## REFERENCES


Anandan, V. K., P. Balamurlidhar, P. B. Rao, A. R. Jain, and C. J. Pan, 2005: An adaptive moments estimation technique applied to MST radar echoes. *J. Atmos. Oceanic Technol.,* **22,** 396–408, doi:10.1175/JTECH1696.1.

Balsley, B. B., and K. S. Gage, 1982: On the use of radars for operational wind profiling. *Bull. Amer. Meteor. Soc.,* **63,** 1009–1018, doi:10.1175/1520-0477(1982)063<1009:OTUORF>2.0.CO;2.

Barth, M. F., R. B. Chadwick, and D. W. van de Kamp, 1994: Data processing algorithms used by NOAA's Wind Profiler Demonstration Network. *Ann. Geophys.,* **12,** 518–528, doi:10.1007/s00585-994-0518-1.

Bianco, L., and J. M. Wilczak, 2002: Convective boundary layer depth: Improved measurement by Doppler radar wind profiler using fuzzy logic methods. *J. Atmos. Oceanic Technol.,* **19,** 1745–1758, doi:10.1175/1520-0426(2002)019<1745:CBLDIM>2.0.CO;2.

Carter, D., K. S. Gage, W. L. Ecklund, W. M. Angevine, P. E. Johnston, A. C. Riddle, J. Wilson, and C. R. Williams, 1995: Development in UHF lower tropospheric wind profiling at NOAA's Aeronomy Laboratory. *Radio Sci.,* **30,** 977–1001, doi:10.1029/95RS00649.

Cornman, L. B., R. K. Goodrich, C. S. Morse, and W. L. Ecklund, 1998: A fuzzy logic method for improved moment estimation from Doppler spectra. *J. Atmos. Oceanic Technol.,* **15,** 1287–1305, doi:10.1175/1520-0426(1998)015<1287:AFLMFI>2.0.CO;2.

Gage, K. S., and B. B. Balsley, 1978: Doppler radar probing of the clear atmosphere. *Bull. Amer. Meteor. Soc.,* **59,** 1074–1093, doi:10.1175/1520-0477(1978)059<1074:DRPOTC>2.0.CO;2.

Hildebrand, P. H., and R. S. Sekhon, 1974: Objective determination of the noise level in Doppler spectra. *J. Appl. Meteor.,* **13,** 808–811, doi:10.1175/1520-0450(1974)013<0808:ODOTNL>2.0.CO;2.

Jordan, J. R., R. J. Lataitis, and D. A. Carter, 1997: Removing ground and intermittent clutter contamination from wind profiler signals using wavelet transforms. *J. Atmos. Oceanic Technol.,* **14,** 1280–1297, doi:10.1175/1520-0426(1997)014<1280:RGAICC>2.0.CO;2.

Klir, G. J., U. H. St. Clair, and B. Yuan, 1997: *Fuzzy Set Theory: Foundations and Applications.* Prentice Hall, 245 pp.

Lehmann, V., and G. Teschke, 2001: Wavelet based methods for improved wind profiler signal processing. *Ann. Geophys.,* **19,** 825–836, doi:10.5194/angeo-19-825-2001.

Lehtinen, R., and J. Jordan, 2006: Improving wind profiler measurements exhibiting clutter contamination using wavelet transforms. Preprints, *WMO Tech. Conf. on Meteorological and Environmental Instruments and Methods of Observation (TECO-2006),* Geneva, Switzerland, WMO, P2.20. [Available online at http://www.wmo.int/pages/prog/www/IMOP/publications/IOM-94-TECO2006/P2(20)_Lehtinen_USA.pdf.]

Mathworks, 2013: MATLAB fuzzy logic toolbox: User's guide. Release R2013b.

Merritt, D. A., 1995: A statistical averaging method for wind profiler Doppler spectra. *J. Atmos. Oceanic Technol.,* **12,** 985–995, doi:10.1175/1520-0426(1995)012<0985:ASAMFW>2.0.CO;2.

Morse, C. S., R. K. Goodrich, and L. B. Cornman, 2002: The NIMA method for improved moment estimation from Doppler spectra. *J. Atmos. Oceanic Technol.,* **19,** 274–295, doi:10.1175/1520-0426-19.3.274.

Passarelli, R. E., P. Romanik, S. G. Geotis, and A. D. Siggia, 1981: Ground clutter rejection in the frequency domain. Preprints, *20th Conf. on Radar Meteorology,* Boston, MA, Amer. Metor. Soc., 295–300.

Riddle, A. C., and W. M. Angevine, 1992: Ground clutter removal from profiler spectra. *Proceedings of the Fifth Workshop on Technical and Scientific Aspects of MST Radar,* B. Edwards, Ed., SCOSTEP Secretariat, University of Illinois, 418–420.

Sato, T., 1989: Radar principles. *Middle Atmosphere Program,* S. Fukao, Ed., Handbook for MAP, Vol. 30, SCOSTEP Secretariat, University of Illinois, 19–53.

Sivanandam, S. N., S. Sumathi, and S. N. Deepa, 2007: *Introduction to Fuzzy Logic Using MATLAB.* Kindle ed. Springer, 430 pp.

Srinivasulu, P., P. Kamaraj, P. Yasodha, M. Durga Rao, and S. Allabakash, 2013: VHF active phased array radar for atmospheric remote sensing at NARL. *Proc. Int. Radar Symp. India 2013,* Banaglore, India, IEEE, 149. [Available online at www.radarindia.com/irsi13papers/13-FP-149.pdf.]

Strauch, R. G., D. A. Merritt, K. P. Moron, K. B. Earnshaw, and D. W. van de Kamp, 1984: The Colorado wind-profiling network. *J. Atmos. Oceanic Technol.,* **1,** 37–49, doi:10.1175/1520-0426(1984)001<0037:TCWPN>2.0.CO;2.

Wilczak, J. M., and Coauthors, 1995: Contamination of wind profiler data by migrating birds: Characteristics of corrupted data and potential solutions. *J. Atmos. Oceanic Technol.,* **12,** 449–467, doi:10.1175/1520-0426(1995)012<0449:COWPDB>2.0.CO;2.

Woodman, R. F., 1985: Spectral moment estimation in MST radars. *Radio Sci.,* **20,** 1185–1195, doi:10.1029/RS020i006p01185.

Zadeh, L. A., 1965: Fuzzy sets. *Inf. Control,* **8,** 338–353, doi:10.1016/S0019-9958(65)90241-X.